Continental response to active ridge subduction

M. Haschke,[1,2] E. R. Sobel,[1] P. Blisniuk,[1] M. R. Strecker,[1] and F. Warkus[1]

[1] Apatite fission track ages from a ~2000 m elevation transect from the Patagonian fold and thrust belt (47.5°S) allow us to quantify the denudational and orographic response of the upper plate to active ridge subduction. Accelerated cooling started at 17 Ma, predating the onset of ridge collision (14–10 Ma), and was followed by reheating between 10 and 6 Ma. Thermal modeling favors reheating on the order of 60°C at ~28°C/Ma due to east-migration of a slab window after the ridge-trench collision. Final rapid cooling since 4 Ma of ~18°C/Ma (geothermal gradient of 14°C/km) correlates with the presence of an orographic barrier and >1 km rock uplift in this region between 17.1 and 6.3 Ma. Increased precipitation and erosion since 4 Ma caused asymmetric exhumation, with 3–4 km on the leeside. Repeated crustal unroofing in response to active ridge subduction can explain the positive gravity anomaly south of the Chile Triple Junction. **Citation:** Haschke, M., E. R. Sobel, P. Blisniuk, M. R. Strecker, and F. Warkus (2006), Continental response to active ridge subduction, *Geophys. Res. Lett.*, *33*, L15315, doi:10.1029/2006GL025972.

1. Introduction

[2] Late Cenozoic rapid uplift and denudation of the southern Patagonian Andes (Figure 1) are linked to subduction of active spreading ridge segments and tectonic shortening [e.g., *Ramos*, 2005], yet the sequential timing and consequences of these processes are poorly constrained. Debate centers on the time of onset and rate of exhumation relative to foreland deformation in the fold and thrust belt, and on the effect of unroofing the Patagonian batholith on the crustal architecture during active ridge subduction [*Ramos*, 1989; *Suárez et al.*, 2000; *Thomson et al.*, 2001; *Folguera and Ramos*, 2002]. Subduction of the Nazca plate north of the Chile triple junction (CTJ) at 46°30′S (Figure 1) is associated with a lower topography (up to 2300 m elevation), little basement exposure, small amounts of late Cenozoic molasse sedimentary rocks east of the topographic divide, and lack of a fold and thrust belt. South of the CTJ, the topography is higher (up to 4070 m) with exhumed Patagonian batholith and pre-Jurassic rocks, late Cenozoic molasse sediments, and development of a fold and thrust belt with 25–45 km of shortening [*Ramos*, 2005]. The thermal history of Patagonian igneous rocks should reflect (1) the significant magmatic (arc volcanic gap, adakite emplacement, the generation of OIB plateau basalts [*Gorring et al.*, 1997]) and morphologic changes (deformation and denudation of the Patagonian Cordillera) caused by active ridge subduction, and (2) provide important constraints on changing structural and geophysical properties of the overriding plate.

[3] When apatites cool through their closure temperature in response to exhumation (~110°C for F-rich apatites [*Green et al.*, 1989]), their ages, track lengths and track length distribution can be used to determine the exhumation history of rocks from the upper ~4 km crust [*Gleadow et al.*, 2002]. The use of this method relies on the fact that fission-tracks accumulate over time at a constant rate, and are subsequently shortened and may eventually disappear in response to elevated temperatures. As a result, the track-length distribution is a sensitive monitor of a crystal's thermal history. Annealing of fission tracks occurs in a temperature interval between ~110° and 60°C (partial annealing zone or PAZ), and depends strongly on the chemical composition of the apatites, reflected in the etch pit diameter Dpar [*Donelick et al.*, 1999; *Ketcham et al.*, 1999].

[4] Samples from elevation transects provide key constraints, as their age-elevation sequences allow us to determine exhumation rates using reasonable assumptions about the geothermal gradient. We present new apatite fission-track data from an elevation transect from the ~100 Ma old Cerro Barrancos pluton [*Pankhurst et al.*, 1999; *Suárez and De La Cruz*, 2001] south of the CTJ at 47°30′S (Figure 1) to quantify the response of the upper plate to active ridge subduction. The results have important implications for mass transfer calculations in the light of recent studies suggesting repeated active ridge subduction for Patagonia during the last 80 Myr [*Flint et al.*, 1994; *Skarmeta and Castelli*, 1997; *Ramos*, 2005], as it implies significant unroofing of the Patagonian Andes which may have affected the geophysical properties of this continental margin segment.

2. Geologic Setting

[5] Previous published thermochronologic data between 47° and 48°S [*Thomson et al.*, 2001] indicate accelerated cooling related to exhumation between 30 and 23 Ma, migrating 180 km eastward to the present-day Cordilleran topographic divide until 12 to 8 Ma due to subduction erosion [e.g., *Bourgois et al.*, 1996]. However, contractional deformation between 18 to 8 Ma predates the Chile Rise collision between 47° and 49°S [*Ramos and Kay*, 1992; *Suárez et al.*, 2000; *Ramos*, 2005], and therefore much shortening, exhumation and subduction erosion must have occurred prior to active ridge subduction [*Folguera and Ramos*, 2002]. Following initial ridge subduction, both

[1]Institut für Geowissenschaften, Universität Potsdam, Potsdam, Germany.
[2]Now at Department of Earth, Ocean and Planetary Sciences, Cardiff University, Park Place, Cardiff CF10 3YE, UK.
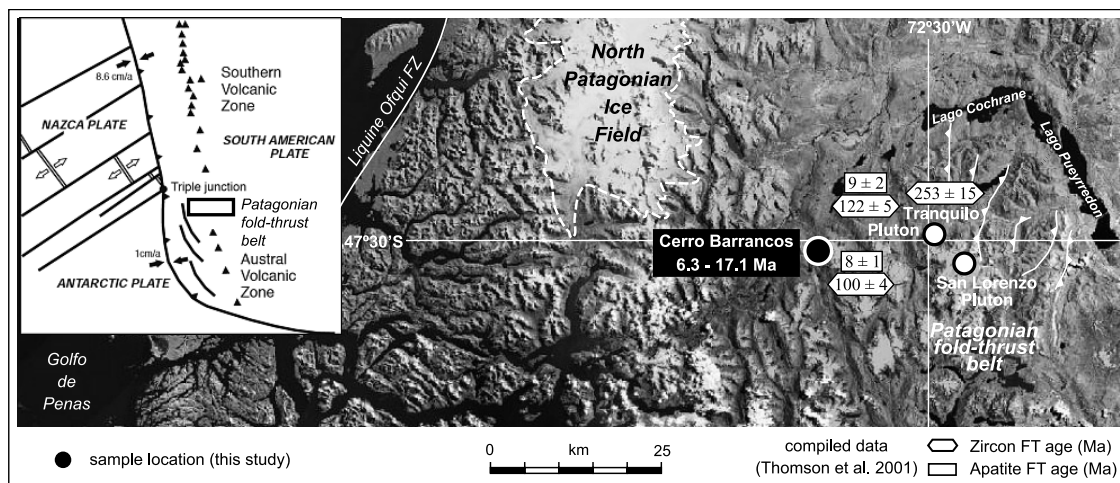
Figure 1. Landsat image of Southern Patagonia at 47°30′S. Black circle indicates location of Cerro Barrancos elevation transect relative to the Patagonian fold and thrust belt (white checked lines). White rectangles and diamonds are compiled apatite and zircon fission track ages from *Thomson et al.* [2001]. Inset shows the plate kinematics of the triple junction between the Antarctic, Nazca and South America plates (adapted from *Ramos* [2005]).

subduction erosion and deformation in the eastern fold and thrust belt [*Suárez et al.*, 2000; *Ramos*, 2005] ceased.

3. Apatite Fission Track Results

[6] Five monzogranitic samples were collected along a 1850 m subvertical elevation transect (Figure 1); four samples between 130 and 1410 m elevation on the western flank and the fifth sample, due to limited accessibility, at 1960 m elevation on the eastern side of the mountain. All samples pass the χ^2 test, indicating that the crystals within each sample represent a consistent thermal history. The cooling ages range from 6.3 ± 0.6 Ma to 17.1 ± 1.2 Ma (Table 1) and increase with elevation (Figure 2). Mean track lengths between 12.88 and 10.30 μm (decreasing with higher elevation from 130 to 1960 m) indicate residence within the apatite partial annealing zone. Some samples show bimodal track length distributions (Figure S1 of the auxiliary material[1]) suggesting reheating followed by final cooling to surface temperatures. Track-length thermal modeling provides a quantitative evaluation of the annealing behavior of a specific sample [*Ketcham et al.*, 1999]. The etch pit diameter Dpar [*Donelick et al.*, 1999] was measured for 20 analyzed crystals per sample (2.20–2.35 μm). Apatites with high Dpar values indicate apatites with moderate

amounts of Cl, suggesting higher closure temperatures of 120°C or higher [*Ketcham et al.*, 1999].

4. Thermal Modeling

[7] We systematically tested a range of likely thermal models to delineate possible cooling histories which can explain the track-length data. Thermal modeling was done using 4 and 5 constraints on the modeled time-temperature paths using the AFTSolve program [*Ketcham et al.*, 2000] and the multicompositional annealing model of *Ketcham et al.* [1999]. The results of the latter are described herein, those of the former yielded similar results. The assemblage of good-fitting model results indicate families of likely thermal histories (Figures 3a–3f). Model runs began at 100 Ma, between 225 and 275°C, consistent with a zircon fission track age of a nearby intrusion of ∼100 Ma [*Thomson et al.*, 2001] (Figure 1), and ended at the present at temperatures between 5 and 15°C. The 3 intermediate constraints were shifted systematically such that possible reheating events could be examined. The 2nd constraint was placed at 16 and 26 Ma, between 50 and 180°C. The 3rd constraint was placed at 6, 8, 10, 12 and 16 Ma, at temperatures between 40 and 180°C, to account for the assumed time of ridge collision (∼14–10 Ma) and induced

Table 1. Summary of Apatite Fission Track Data[a]

Sample ID	Elevation, m	Latitude, S	Longitude, W	Number of Crystals	P(χ)², %	Age, Ma	±1 σ	Length, μm	±1 σ	n	Dpar, μm	SD
CB-1960	1960	47°33.56′	72°46.22′	28	99	17.1	1.2	10.30	0.24	106	2.35	0.20
CB-1410	1410	47°33.80′	72°49.29′	27	92	11.3	0.7	11.94	0.29	111	2.34	0.15
CB-930	930	47°33.82′	72°50.04′	26	99	11.0	1.1	12.74	0.30	104	2.20	0.20
CB-550	550	47°33.85′	72°50.84′	26	100	7.3	0.7	12.88	0.29	106	2.33	0.17
CB-130	130	47°34.22′	72°51.92′	29	99	6.3	0.6	12.10	0.33	101	2.33	0.16

[a]Samples were irradiated at Oregon State University, USA. Analyses were performed by F. Warkus using methodology described by *Sobel and Strecker* [2003]. The pooled age is reported for all samples as they pass the χ^2 test; error is 1σ, calculated using a zeta of 370.1 ± 6.1 for apatite [*Warkus*, 2002]. P(χ)² [%] = χ^2 probability. Values greater than 5% are considered to pass this test and represent a single age population. n = number of tracks counted for track length measurements. Dpar = etch pit diameter [*Donelick et al.*, 1999], SD = standard deviation.

[1]Auxiliary material data sets are available at ftp://ftp.agu.org/apend/gl/2006gl025972. Other auxiliary material files are in the HTML.
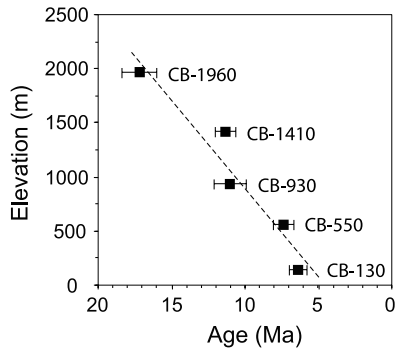
Figure 2. Apatite fission track ages versus sample elevation. Note linear trend of higher fission track ages with increasing sample elevation.

reheating. The 4th constraint was positioned between 4 and 1 Myr later than the 3rd constraint, at temperatures between 60 and 180°C, to constrain the onset and rate of cooling after reheating (Table S1).

[8] Models were run using the constrained random search algorithm, with 20,000 monotonic heating or cooling paths and two halvings between adjacent constraints. This strategy produced 55 models per sample with good or acceptable-fitting results (Figures 3a–3f). Samples CB130 and CB1410 both yielded good-fitting models (2 σ fits) for most constraints except when final cooling commenced at 4 Ma; samples CB550 and CB930 produced acceptable models (1 σ fits). Comparing the best fits from all of the good fitting models for samples CB130 and CB 1410 shows that the 2 samples behave quite similarly: the amount of reheating is 65 and 53°C at average rates of 28 and 27°C/Ma while the final cooling is 137 and 119°C at average rates of 20 and 16°C/Ma (standard deviation of the amounts and rates of reheating: ~24°C and 20°C/Myr). The final cooling is better constrained, with standard deviations of ~10 and 5 for the amount and rate, respectively. Using the averaged best-fit peak reheating temperatures, the geothermal gradient is 14°C/km. Sample CB1960 yielded acceptable fits for this modeling strategy, yet the shape of the length distribution is different, suggesting reheating or cooling in a different manner, possibly reflecting a markedly different, drier exhumation history than the more humid windward side.

5. Exhumation History

[9] The emplacement of the Cerro Barrancos pluton at ~100 Ma was followed by regional cooling until the late Cenozoic. Between 17 and 6 Ma, we estimate a minimum of 3–4 km of exhumation at rates of 600–650 m/Ma. Interestingly, the onset of accelerated exhumation (~17 Ma,

Figure 4) predates the time of ridge collision (14–10 Ma), which rules out subduction of active spreading segments as the main trigger mechanism for denudation. Thus the thermochronometric results may reflect a combination of
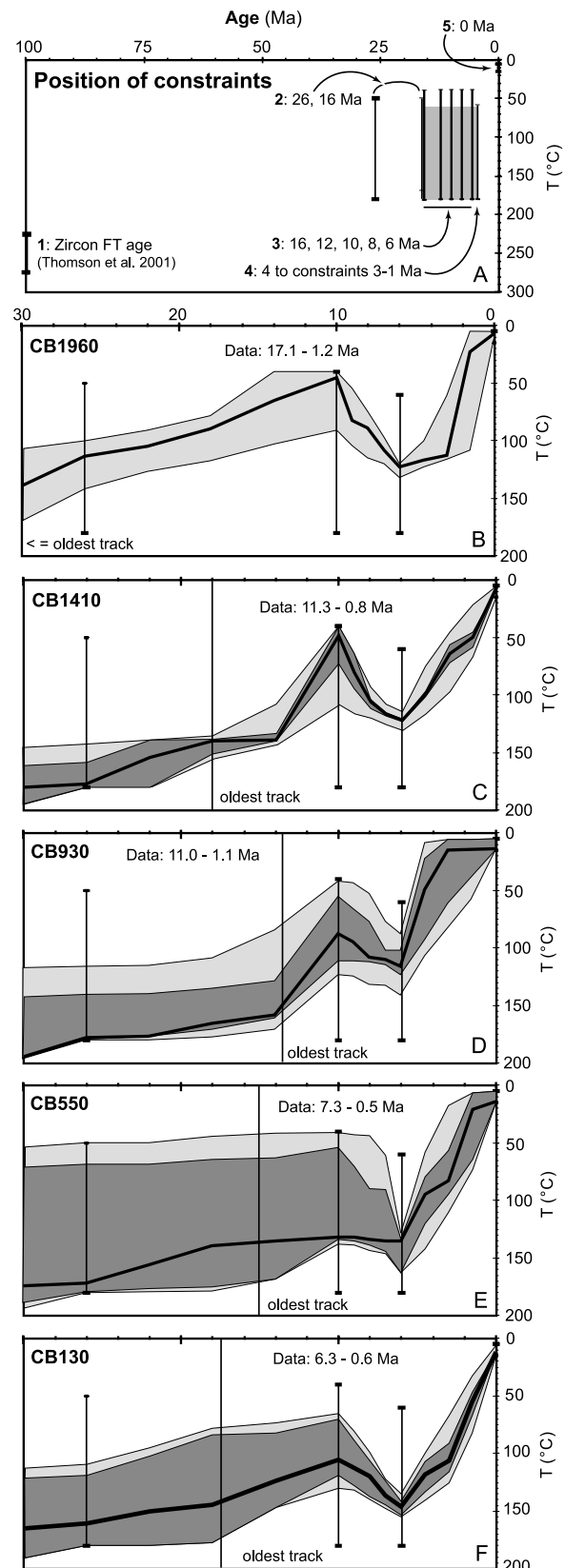
Figure 3. Representative AFTSolve thermal modeling results for all 5 samples (conducted by Ed Sobel) showing a possible thermal history. Dark and light grey shading indicate good and acceptable fits, respectively. (a) Schematic diagram illustrating positions of constraints; (b) model results for sample CB 1960; (c) model results for sample CB 1410; (d) model results for sample CB 930; (e) model results for sample CB 550; (f) model results for sample CB 130. *Blisniuk et al.* (2006).
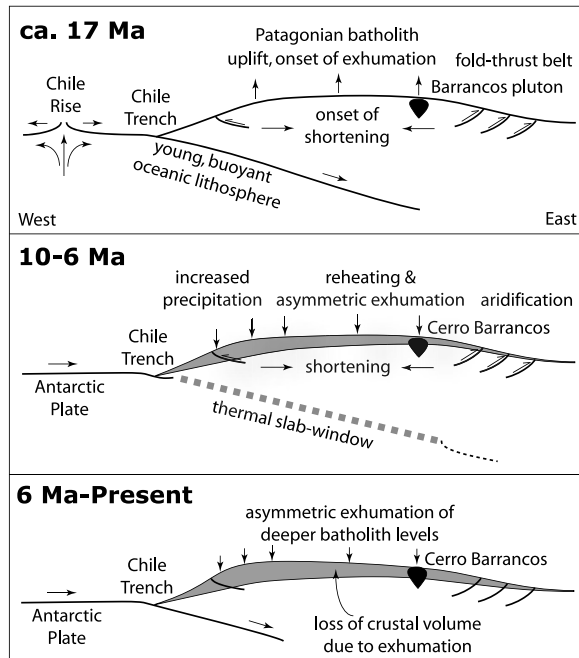
Figure 4. Cross sections (west-east) showing the continental response to active ridge subduction in southern Patagonia (see text for discussion).

subduction erosion and eastward propagation of the eastern fold and thrust belt. Similar patterns of eastward propagating deformation fronts are known from the central Andes [*Allmendinger et al.*, 1997]. They can be attributed to along-strike variation in the horizontal tectonic forces acting across the plate boundary [*Wdowinski and Bock*, 1994; *Pope and Willet*, 1998] and changes in the mantle flow field [*Russo and Silver*, 1996]; both are consequences which are anticipated during active ridge subduction.

[10] Late Cenozoic subduction erosion and pre ~14 Ma cooling combined are consistent with retroarc transpressive shortening between ~18–8 Ma [*Ramos*, 2005], and caused thrust-related, eastward migration of the locus of maximum denudation in the Patagonian fold and thrust belt, as young and buoyant oceanic lithosphere approached the trench in a regime of low partitioning [*Folguera and Ramos*, 2002] (Figure 4). Between ca. 10 and 6 Ma, the data indicate an episode of reheating of 60 ± 30°C (Figures 3a–3f). Although not well constrained, reheating must have terminated before 4 Ma and was most likely caused by eastward migration of a subducting slab-window when asthenosphere from beneath the subducted Chile Ridge came into contact with the base of the overriding South American plate [*Ramos and Kay*, 1992; *Gorring et al.*, 1997; *Ramos*, 2005] (Figure 4). Final cooling commenced at ~4 Ma when the samples were exhumed to the surface at a higher rate than during the previous regional cooling.

6. Discussion

[11] The thermochronologic data presented is consistent with changes in oxygen and carbon isotope compositions of pedogenic carbonate nodules, and increasing sediment flux and deposition rates [*Blisniuk et al.*, 2006]. Both indicate >1 km of effective surface uplift of this Cordilleran segment

between ~17 and 14 Ma, aridification of the eastern foreland and increased precipitation rates on the western flank of the Patagonian Andes (Figure 4).

[12] Alternatively, reheating of the Cerro Barrancos pluton could be explained by tectonic and/or sedimentary basin burial, but there are neither structural data to support burial of this intrusion beneath a Miocene thrust fault, nor evidence to support burial beneath a several km-thick Miocene sedimentary basin. Another possibility is igneous activity near the sampling area, yet the closest intrusion (San Lorenzo pluton, Figure 1) has an emplacement age of 6.5 Ma [*Welkner and Suárez*, 1999; *Suárez and De La Cruz*, 2001] which is too young to explain reheating at ~10 Ma.

[13] Asymmetric exhumation of the upper plate, on the order of 4–9 km in the west [*Thomson et al.*, 2001] and 3–4 km in the east, in conjunction with ~200 km of eastward progressing subduction erosion, imply a major loss in continental crustal volume, orogenic narrowing and exhumation of deeper and denser rocks of the Patagonian batholith. These figures may even be considered minimum, as recent work considers at least three episodes of active ridge subduction during the late Cretaceous, Eocene and late Miocene [*Flint et al.*, 1994; *Skarmeta and Castelli*, 1997; *Ramos*, 2005]. This must have caused crustal stacking and repeated episodes of exhumation of the Patagonian forearc. Unroofing of this order of magnitude may explain, at least in part, some changing geophysical properties north and south of the present CTJ. North of the CTJ, the forearc and arc regions show neutral gravity [*Murdie et al.*, 2000], whereas south of the CTJ they show a significant positive gravity anomaly along the forearc and batholith [*Murdie et al.*, 2000] which may indicate the presence of higher density basement rocks. Therefore the positive gravity anomaly may reflect the asymmetric unroofing pattern of the Patagonian batholith upon late Cenozoic active ridge subduction, as described and quantified in this study. Figures of exhumation in this order of magnitude may be typical of continental margins responding to active ridge subduction, and provide estimates for crustal mass transfer calculations.

References

Allmendinger, R. W., T. E. Jordan, S. M. Kay, and B. L. Isacks (1997), The evolution of the Altiplano-Puna plateau of the central Andes, *Annu. Rev. Earth Planet. Sci.*, *25*, 139–174.

Blisniuk, P. M., L. A. Stern, C. P. Chamberlain, P. K. Zeitler, V. A. Ramos, E. R. Sobel, M. Haschke, M. R. Strecker, and F. Warkus (2006), Links between mountain uplift, climate, and surface processes in the southern Patagonian Andes, in *The Andes - Active Subduction Orogeny: Frontiers in Earth Sciences*, edited by O. Oncken, G. Chong, G. Franz, P. Giese, H.-J. Götze, V. Ramos, M. Strecker, and P. Wigger, Springer Verlag, in press.

Bourgois, J., H. Martin, Y. Lagabrielle, J. Le Moigne, and J. Frutos Jara (1996), Subduction erosion related to spreading ridge subduction: Taitao Peninsula (Chile margin triple junction area), *Geology*, *24*, 723–726.

Donelick, R. A., R. A. Ketcham, and W. D. Carlson (1999), Variability of apatite fission-track annealing kinetics: II. Crystallographic orientation effects, *Am. Mineral.*, *84*, 1224–1234.

Flint, S. S., D. J. Prior, S. M. Agar, and P. Turner (1994), Stratigraphic and structural evolution of the Tertiary Cosmelli basin and its relationship to the Chile triple junction, *J. Geol. Soc.*, *151*, 251–268.

Folguera, A., and V. A. Ramos (2002), Particion de la deformacion durante el Neogeno en los Andes Patagonicos Septentrionales (37°–46°S), *Rev. Soc. Geol. Esp.*, *15*, 81–93.

Gleadow, A. J., D. X. Belton, B. P. Kohn, and R. W. Brown (2002), Fission track dating of phosphate minerals and the thermochronology of apatite, in *Phosphates: Geochemical, Geobiological, and Materials Importance*, *Rev. Mineral. Geochem.*, vol. 48, edited by M. J. Kohn, J. Rakovan, and J. M. Hughes, pp. 579–630, Mineral. Soc. of Am., Washington, D. C.

Gorring, M. L., S. M. Kay, P. K. Zeitler, V. A. Ramos, D. Rubilio, M. I. Fernandez, and J. L. Panza (1997), Neogene Patagonian plateau lavas: Continental magmas associated with ridge collision at the Chile Triple Junction, *Tectonics*, *16*, 1–17.

Green, P. F., I. R. Duddy, G. M. Laslett, K. A. Hegarty, A. J. Gleadow, and J. F. Lovering (1989), Thermal annealing of fission tracks in apatite, 4. Quantitative modelling techniques and extension to geological time-scales, *Chem. Geol.*, *79*, 155–182.

Ketcham, R. A., R. A. Donelick, and W. D. Carlson (1999), Variability of apatite fission-track annealing kinetics: III. Extrapolation to geological time scales, *Am. Mineral.*, *84*, 1235–1255.

Ketcham, R. A., R. A. Donelick, and M. B. Donelick (2000), AFTSolve: A program for multikinetic modeling of apatite fission-track data, *Geol. Mater. Res.*, *2*, 1–32.

Murdie, R. E., P. Styles, D. J. Prior, and A. J. Daniel (2000), A new gravity map of southern Chile and its preliminary interpretation, *Rev. Geol. Chile*, *27*(1), 49–63.

Pankhurst, R. J., S. D. Weaver, F. Hervé, and P. Larrando (1999), Mesozoic-Cenozoic evolution of the North Patagonian Batholith in Aysén, southern Chile, *J. Geol. Soc. London*, *156*, 673–694.

Pope, D. C., and S. D. Willet (1998), Thermal mechanical model for crustal thickening in the central Andes driven by ablative subduction, *Geology*, *26*, 511–514.

Ramos, V. A. (1989), Andean foothills structures in northern Magallanes Basin, Argentina, *AAPG Bull.*, *73*, 887–903.

Ramos, V. A. (2005), Seismic ridge subduction and topography: Foreland deformation in the Patagonian Andes, *Tectonophysics*, *399*, 73–86.

Ramos, V. A., and S. M. Kay (1992), Southern Patagonian plateau basalts and deformation: Backarc testimony of ridge collisions, *Tectonophysics*, *205*, 261–282.

Russo, R. M., and P. G. Silver (1996), Cordillera formation, mantle dynamics and the Wilson cycle, *Geology*, *24*, 511–514.

Skarmeta, J., and J. C. Castelli (1997), Intrusion sintectonica del granito de Las Torres del Paine, Andes Patagonicos de Chile, *Rev. Geol. Chile*, *24*, 55–74.

Sobel, E. R., and M. R. Strecker (2003), Uplift, exhumation, and precipitation: Tectonic and climatic control of late Cenozoic landscape evolution in the northern Sierras Pampeanas, Argentina, *Basin Res.*, *15*, doi:10.1046/j.1365-2117.2003.00214.x, p. 431–451.

Suárez, M., and R. De la Cruz (2001), Jurassic to Miocene K-Ar dates from eastern central Patagonian Cordillera plutons, Chile (45°–48°S), *Geol. Mag.*, *138*, 53–66.

Suárez, M., R. De La Cruz, and C. M. Bell (2000), Timing and origin of deformation along the Patagonian fold and thrust belt, *Geol. Mag.*, *137*, 345–353.

Thomson, S. N., F. Hervé, and B. Stöckhert (2001), Mesozoic-Cenozoic denudation history of the Patagonian Andes (southern Chile) and its correlation to different subduction processes, *Tectonics*, *20*, 693–711.

Warkus, F. (2002), Die neogene Hebungsgeschichte der Patagonischen Anden im Kontext der Subduktion eines aktiven Spreizungszentrums, doctoral thesis, 99 pp., Univ. of Potsdam, Potsdam, Germany.

Wdowinski, S., and Y. Bock (1994), The evolution of deformation and tomography of high elevated plateaus: 2. Application to the central Andes, *J. Geophys. Res.*, *99*, 7121–7130.

Welkner, D., and M. Suárez (1999), Los plutones del área del Cerro San Lorenzo (47°30′S): Valores K–Ar y Ar–Ar, *Actas Congr. Geol. Argent.*, *XIV*, 112–113.

_____

P. Blisniuk, E. R. Sobel, M. R. Strecker, and F. Warkus, Institut für Geowissenschaften, Universität Potsdam, D-14469 Potsdam, Germany.

M. Haschke, Department of Earth, Ocean and Planetary Sciences, Cardiff University, Park Place, Cardiff CF10 3YE, UK. (haschkem@cardiff.ac.uk)